

# Adaptive and optimal detection of elastic object scattering with single-channel monostatic iterative time reversal\*

Ying Ying-Zi(应英子)<sup>†</sup>, Ma Li(马力), and Guo Sheng-Ming(郭圣明)

*Institute of Acoustics, Chinese Academy of Sciences, Beijing 100190, China*

(Received 4 February 2010; revised manuscript received 24 December 2010)

In active sonar operation, the presence of background reverberation and the low signal-to-noise ratio hinder the detection of targets. This paper investigates the application of single-channel monostatic iterative time reversal to mitigate the difficulties by exploiting the resonances of the target. Theoretical analysis indicates that the iterative process will adaptively lead echoes to converge to a narrowband signal corresponding to a scattering object's dominant resonance mode, thus optimising the return level. The experiments in detection of targets in free field and near a planar interface have been performed. The results illustrate the feasibility of the method.

**Keywords:** iterative time reversal, resonant scattering, echo enhancement

**PACS:** 43.30.+m

**DOI:** 10.1088/1674-1056/20/5/054301

## 1. Introduction

The iterative time reversal in target detection operates in a pulse-echo mode, which resembles the acoustic ping-pong. The technique utilizes a transceiver, which is a transmitter and receiver couple, to initially illuminate the target with a broadband interrogation pulse, then to measure the backscattered wave. A bandpass filter is used to suppress the interfering signal. The preprocessed data stream is reversed in the time domain and retransmit back. The procedures are iterated. Since wave equation of non-dispersive and motionless media supports both time reversal invariance and spatial reciprocity, the iterative time reversal process will gradually lead echoes to converge to a narrowband signal, whose central frequency corresponds to a maximum of the spectral response of the target scattering, thus improving the return level and mitigates the difficulties of noise and reverberation.

The iterative time reversal was initially demonstrated to focus on the most reflective scatterer in the ultrasonic laboratory experiments,<sup>[1,2]</sup> then the concept was extended to the ocean waveguide.<sup>[3]</sup> Reference [4] proposed a real time technique to discriminate between scatterers by using a particular sequence of filtered waves to replace the decomposition of the time reversal operator method.<sup>[5]</sup> Recent work<sup>[6]</sup> used time-reversed reverberation signals iteratively to con-

struct the reflectivity maps of the ocean bottom and to distinguish the bottom or buried targets. All these methods are based on the spatial focusing of acoustic energy with a time-reversal array.

The analysis<sup>[7]</sup> showed that the iterative process involving a time reversal mirror would automatically obtain the optimal incident field to achieve the maximum distinguishability between the target and the background in acoustic imaging. In this study, the single-channel monostatic iterative time reversal mirror will take effect as an adaptive matched filter for the spectral response of the target scattering. We have performed the experiments in detection of elastic objects in tank and at sea.

## 2. Free field circumstance

### 2.1. Single-channel system transfer function in free field

In the free field circumstance, an elastic solid sphere with radius  $a$  immersed in the fluid is taken as the target, which is centred at  $\mathbf{r}_t$  and the transceiver with a point-like model is situated at  $\mathbf{r}_s$ . First, the probe signal is emanated by the transmitter. Then the wave is scattered by the target and eventually received by the receiver. The round trip of the signal

\*Project supported by the Innovation Foundation of Chinese Academy of Sciences (Grant No. CXJJ-260).

<sup>†</sup>Corresponding author. E-mail: yingyz05@mails.gucas.ac.cn

© 2011 Chinese Physical Society and IOP Publishing Ltd

<http://www.iop.org/journals/cpb> <http://cpb.iphy.ac.cn>

could be viewed as going through a linear time invariant system expressed in terms of the backscattering form function,<sup>[8]</sup>

$$h(\omega) := \alpha_e(\omega)\alpha_r(\omega)\frac{a}{2R^2}\exp(2ik_0R)f(\pi;\omega), \quad (1)$$

where  $\alpha_e$  and  $\alpha_r$  are the transmission and the reception acousto-electric transformation coefficients, respectively,  $k_0$  is the wave number in the fluid, and  $R = \|\mathbf{r}_s - \mathbf{r}_t\|$  is the distance between the target and the transceiver. The form function  $f(\theta;\omega)$ , which denotes the steady-state response of the target scattering, is derived by expanding both the incident and secondary scattered field in the spherical polar coordinate and determining the coefficients with appropriate boundary conditions. The problem is investigated in a far field monostatic deployment, that is  $\theta = \pi$ .

## 2.2. Resonant convergence with the iterative process

Assume that  $e_0$  is the initial broadband interrogation pulse, then the backscattered signal is  $e_0h$ . As time reversal conducted in the time domain is equivalent to a phase conjugation in the frequency domain, we use the superscript  $*$  to denote the complex conjugate operator, then the time reversed echo signal of the first iteration is  $e_0^*h^*$ , which is adopted as the input signal for the next illumination. The times reversed echo signal of the second iteration is  $e_0hh^*$  and so on. The renewed input signal after the  $n$ th iteration is

$$e_n(\omega) = \begin{cases} (e_0^*|h|^{n-1}h^*)(\omega), & \text{if } n \text{ is odd,} \\ (e_0|h|^n)(\omega), & \text{if } n \text{ is even.} \end{cases} \quad (2)$$

The signal spectral amplitude is  $|e_n| = |e_0||h|^n$  for both cases. The normalized form, which is divided by its maximum, converges to

$$\lim_{n \rightarrow \infty} \frac{|e_n(\omega)|}{\max\{|e_n(\omega)|\}} = \mathbf{1}_{\{\omega: \omega=\omega_0\}}(\omega), \quad (3)$$

where the indicator function of the set  $A$  is  $\mathbf{1}_A(\omega) = 1$  if  $\omega \in A$ , and  $\mathbf{1}_A(\omega) = 0$  if  $\omega \in A^c$ . The  $\omega_0$  is the frequency corresponding to a maximum of the amplitude of the system transfer function

$$\omega_0 := \arg \max_{\omega \in [\omega_1, \omega_2]} |h(\omega)|, \quad (4)$$

where the frequency interval  $[\omega_1, \omega_2]$  is defined by a bandpass filter. We always select the band in a flat or a monotone domain of the transceiver response  $|\alpha_e\alpha_r|$ , which may also be calibrated, otherwise the signal may

converge to a peak of the transceiver response. Thus the converged frequency approximates to

$$\omega_0 \approx \arg \max_{\omega \in [\omega_1, \omega_2]} |f(\pi; \omega)|. \quad (5)$$

Equation (3) denotes that the returned echoes will gradually converge to a narrowband signal, which corresponds to a resonance mode according to Eq. (5). The narrowband signal causes eigenvibration of the elastic object and enhances the return level. The form function could be regarded as the fingerprint of the target. The iterative time reversal process will locate the maxima of the form function. This signature could be used for classification and identification purposes.

## 2.3. Tank experimental results

In the tank experiment, a transceiver and an aluminium sphere with 5 cm in radius are suspended at the same depth. The interrogation pulse synthesized by a programmable signal generator is emanated by the transceiver in transmission mode. The echo is received by the transceiver in reception mode, then is recorded by an oscilloscope. The signal generator and the oscilloscope are linked to a PC through an USB connector and a twisted-pair cable, respectively.

The form function is the inherent characteristics of the object, which is mainly determined by its particular geometry and material composition. Figure 1 shows the modulus of the backscattering form function of the aluminium sphere, including both the theoretical and the measured results. It demonstrates the strong fluctuation behaviour existing even for the regular shape of a sphere. The strong fluctuation is caused by the superposition of narrow resonances in individual partial waves.<sup>[9]</sup> The converged frequency of the iterative time reversal process corresponds to a resonance mode of the elastic object. By changing the

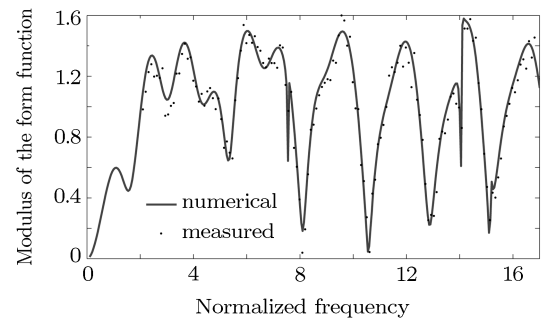


**Fig. 1.** Fluctuation in the modulus of the form function of the aluminium sphere with 5 cm in radius, plotted versus dimensionless frequency.

central frequency of the initial interrogation pulse and adjusting the corresponding parameters of the band-

pass filter. Figures 2(a) and 2(b) illustrate two converged echoes and their respective spectral amplitudes. One converged frequency is 12.5 kHz, which corresponds to a resonance peak about at  $k_0 a = 2.55$  and the other is 56.5 kHz, which approximates to a maximum at  $k_0 a = 12$ . The bias is mainly introduced by the slope of the transceiver frequency response and the ripples in the pass band of the filter. The Gibbs oscillation might arise in the process of cutting the echoes with a rectangular window.

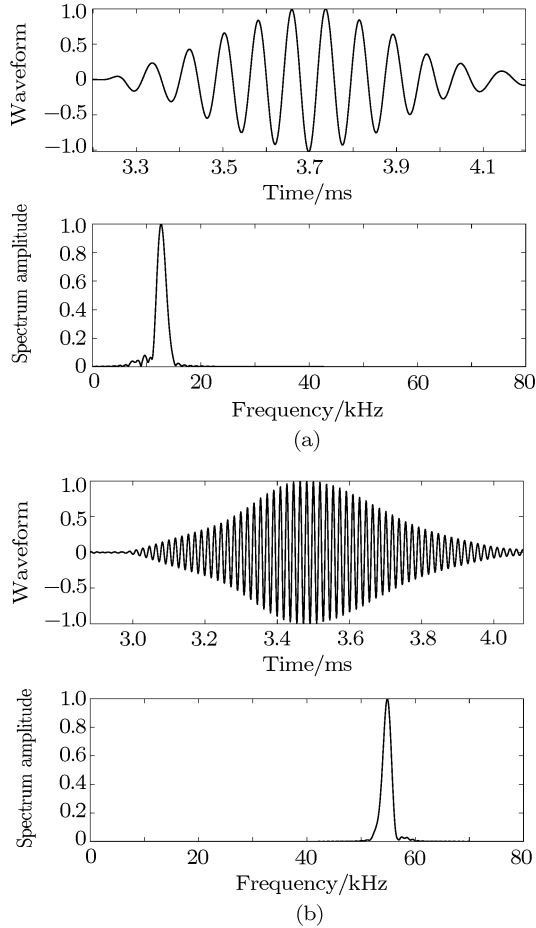


**Fig. 2.** (a) Converged echo and respective spectral amplitude with a 2-cycle continuous wave (CW) of 10 kHz central frequency as the initial probe signal and the converged frequency is 12.5 kHz, (b) by changing the probe frequency to 55 kHz, the converged frequency is shifted to 56.5 kHz.

Figures 3(a) and 3(b) show total signals recorded by the transceiver of the 1st and the 8th iteration. The first envelopes are the normalized transmitting signals picked up by the transceiver directly and the second envelopes are the echoes scattered by the target. The target return level of the 8th iteration is enhanced in comparison with that of the 1st iteration. As spectral

narrowing corresponds to time-domain extension, the echo waveform will gradually be prolonged.

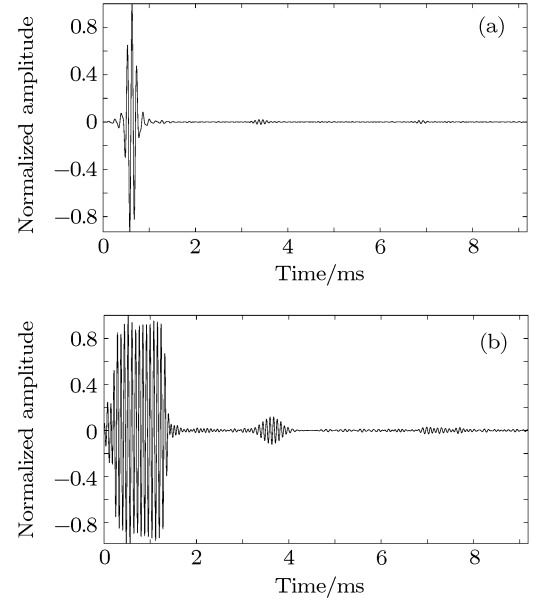


**Fig. 3.** Total signals recorded by the receiver with a 2-cycle CW of 10 kHz central frequency as the initial interrogation pulse. (a) The 1st iteration, (b) the 8th iteration.

### 3. Near interface circumstance

#### 3.1. Target scattering in the presence of interface reverberation

As depicted in Fig. 4(a), the experiment in detection of a target near a planar interface is in a single-channel monostatic configuration, where the elastic object is resting on the sea floor and the transceiver is located right above it.

The boundary conditions of the elastic object and the saturated sea are the continuity of the normal components of displacement and surface traction and the inner tangential of surface traction vanishes. On  $\partial D_1 \cup \partial D_2$ ,

$$\mathbf{n} \cdot \mathbf{u}_- = \mathbf{n} \cdot \mathbf{u}_+, \quad \mathbf{n} \cdot \mathbf{t}_- = \mathbf{n} \cdot \mathbf{t}_+, \quad \mathbf{n} \times \mathbf{t}_- = 0, \quad (6)$$

where  $\mathbf{n}$  is the normal of the surface pointing outward and the plus and minus signs denote the boundary values taken from outside and inside, respectively.

Since the scattered pressure field in the fluid is our interested quantity, we will find the radiating solution  $p \in C^2(\mathbb{R}^3 \setminus (\bar{D}_1 \cup \bar{D}_2))$  giving a continuous functions on  $\partial D_1 \cup \partial D_2$ . The Helmholtz–Kirchhoff integral representations of the fields in each domain are adopted with the null-field hypothesis:

$$\begin{aligned}
 & \int_{\partial D_1 \cup \partial D_2} \{p_+(\mathbf{r}') \mathbf{n}(\mathbf{r}') \cdot \nabla' g(\mathbf{r}, \mathbf{r}') - \lambda_0 k_0^2 g(\mathbf{r}, \mathbf{r}') \mathbf{n}(\mathbf{r}') \cdot \mathbf{u}_-(\mathbf{r}')\} ds(\mathbf{r}') \\
 &= \begin{cases} p(\mathbf{r}) - p^{\text{in}}(\mathbf{r}) = p^{\text{sc}}(\mathbf{r}), & \mathbf{r} \in \mathbb{R}^3 \setminus (\bar{D}_1 \cup \bar{D}_2), \\ -p^{\text{in}}(\mathbf{r}), & \mathbf{r} \in D_1 \cup D_2, \end{cases} \quad (7)
 \end{aligned}$$

$$\begin{aligned}
 & \int_{\partial D_i} \{-p_+(\mathbf{r}') \mathbf{n}(\mathbf{r}') \cdot \mathbf{G}(\mathbf{r}, \mathbf{r}') - \mathbf{u}_-(\mathbf{r}') \cdot [\mathbf{n}(\mathbf{r}') \cdot \mathbf{\Sigma}(\mathbf{r}, \mathbf{r}')]\} ds(\mathbf{r}') \\
 &= \begin{cases} \mathbf{u}(\mathbf{r}), & \mathbf{r} \in D_i, \\ 0, & \mathbf{r} \in \mathbb{R}^3 \setminus \bar{D}_i, \quad i = 1, 2, \end{cases} \quad (8)
 \end{aligned}$$

where  $\lambda_0$  is the bulk modulus of the fluid,  $g$  is the scalar Green's function,  $\mathbf{G}$  and  $\mathbf{\Sigma}$  are the Green's displacement dyadic and Green's stress triadic for an unbounded region, respectively.

Through the integral equations and the boundary conditions, the scattered field can be solved numerically with the  $T$ -matrix formalism, the boundary element method, the finite element method, etc. If an unit-amplitude monochromatic signal is applied to the omnidirectional point source, the incident pressure field is

$$\begin{aligned}
 p^{\text{in}}(\mathbf{r}) &= \frac{\exp(ik_0|\mathbf{r} - \mathbf{r}_s|)}{|\mathbf{r} - \mathbf{r}_s|} \\
 (\mathbf{r} \in \mathbb{R}^3 \setminus \{\mathbf{r}_s\}, \text{ and } \mathbf{r}_s \in \mathbb{R}^3 \setminus (\bar{D}_1 \cup \bar{D}_2)). \quad (9)
 \end{aligned}$$

The system transfer function equals the scattered pressure field received at the same position in Eq. (7), that is

$$h(\omega) = p^{\text{sc}}(\mathbf{r}_s; \omega). \quad (10)$$

The scattering of a target near a planar waveguide boundary is a multiple scattering process, which may result in the super-resonant phenomenon and approach the greatest return near normal incidence.<sup>[10]</sup>

### 3.2. At-sea experimental results

At-sea experiment has been performed in the Yellow Sea, China. A 2-cycle continuous wave of 15 kHz central frequency is emanated as the initial interrogation pulse. Figure 4(b) illustrates the normalized spectra of the echoes of the first nine iterations. At the beginning of the process, the echo frequency content is expanded. When the iteration number increases, the echoes will gradually converge to a narrowband signal. The response peak of the transceiver is avoided by adjusting the bandpass filter in the flat response interval.

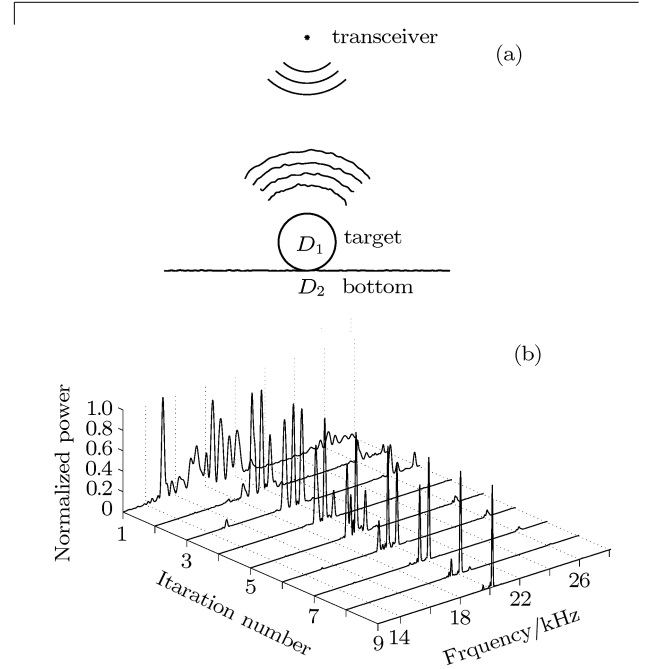


**Fig. 4.** (a) Geometric configuration of the at-sea experiment, symbol \* denotes the transceiver and the elastic object is labeled as  $D_1$ , while  $D_2$  is the sea bottom; (b) echo frequency components of the first nine iterations.

In the absence of target, the same procedure with a similar iteration number will not result in the resonant convergence, as the flat sea floor has no sharp and dominant frequency response. We judge the existence of target by this acoustic signature.

## 4. Summary

The iterative process involving a single-channel time reversal mirror will automatically turn the frequency of the interrogation signal to an optimized one that matches the target resonant scattering, thus maximize the echo return level. The method is based on feature extraction rather than the energy flux, so we only need to examine the converged state of the iterative process instead of resolving the target scattering signal from the background reverberation. The experimental results also illustrate that it is capable of being noise tolerated to a certain degree.

## References

- [1] Prada C, Wu F and Fink M 1991 *J. Acoust. Soc. Am.* **90** 1119
- [2] Prada C, Thomas J L and Fink M 1995 *J. Acoust. Soc. Am.* **97** 62
- [3] Song H C, Kuperman W A, Hodgkiss W S, Akal T and Ferla C 1999 *J. Acoust. Soc. Am.* **105** 3176
- [4] Montaldo G, Tanter M and Fink M 2004 *J. Acoust. Soc. Am.* **115** 776
- [5] Prada C, Manneville S, Spoliansky D and Fink M 1996 *J. Acoust. Soc. Am.* **99** 2067
- [6] Sabra K G, Roux P, Song H C, Hodgkiss W S, Kuperman W A, Akal T and Stevenson J M 2006 *J. Acoust. Soc. Am.* **120** 1305
- [7] Isaacson D, Cheney M and Lassas M 2001 *SIAM J. Appl. Math.* **61** 1628
- [8] Hickling R 1962 *J. Acoust. Soc. Am.* **34** 1582
- [9] Flax L, Dragonette L R and Überall H 1978 *J. Acoust. Soc. Am.* **63** 723
- [10] Bishop G C and Smith J 1999 *J. Acoust. Soc. Am.* **105** 130